Journal of Physics: Conference Series

PAPER • OPEN ACCESS

Innovative rail transport of a supersized land-based wind turbine blade

To cite this article: William Scott Carron and Pietro Bortolotti 2020 *J. Phys.: Conf. Ser.* **1618** 042041

View the article online for updates and enhancements.

You may also like

- Comparing wind turbine aeroelastic response predictions for turbines with increasingly flexible blades
Kathy Cao, Kelsey Shaler and Nick Johnson

- On the Improvement of Convergence Performance for Integrated Design of Wind Turbine Blade Using a Vector Dominating Multi-objective Evolution Algorithm
L Wang, T G Wang, J H Wu et al.

- Mechanism and Mitigation Strategy of Sub-synchronous Oscillation Caused by Grid-connected DFIG with Series Compensation
Jing Yang, Yong Sun, Ladier Fa et al.

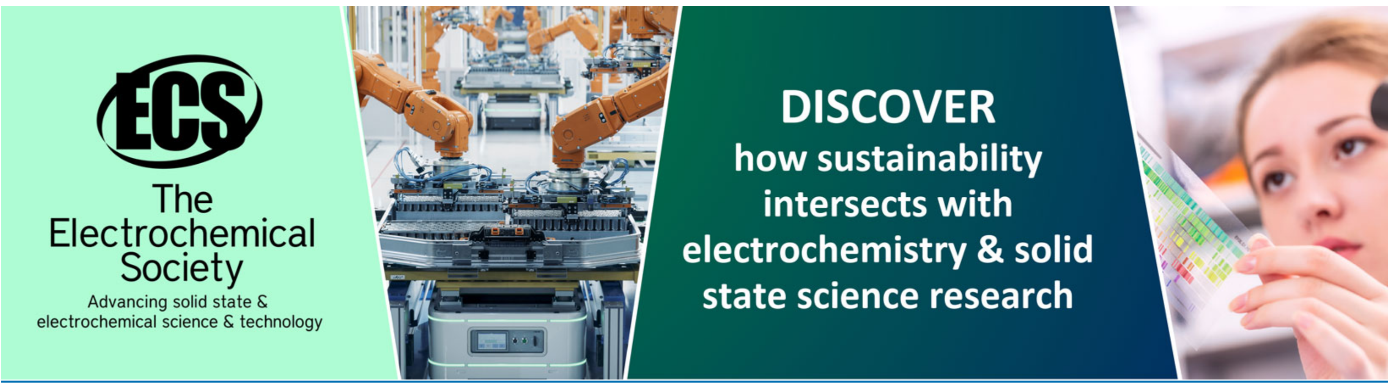

This content was downloaded from IP address 3.139.240.142 on 05/05/2024 at 08:18

Innovative rail transport of a supersized land-based wind turbine blade

William Scott Carron[1], **Pietro Bortolotti**[1]

[1] National Renewable Energy Laboratory, Boulder, Colorado

E-mail: `william.carron@nrel.gov`
Keywords: Rail transport, Blade logistics, Transportation barrier, Blade scaling, Supersized blades, MDAO, System optimization, Rotor design, Blade design

Abstract. Wind turbine blade logistic providers are being challenged with escalating costs and routing complexities as one-piece blade approach lengths of 75 m in various regions of the U.S. land-based market. New lower cost solutions are needed to enable further reductions in the levelized cost of energy (LCOE) and continued market expansion. In this paper, a novel method of using existing U.S. rail infrastructure to deploy 100-m, one-piece blades to U.S. land-based wind sites is numerically investigated. The study removes the constraint that blades must be kept rigid during transport, and it allows bending to keep blades within a clearance profile while navigating horizontal and vertical curvatures. Novel system optimization and blade design processes consider blade structural constraints and rail logistic constraints in parallel to develop a highly flexible, rail-transportable blade. Results indicate maximum deployment potential in the Interior region of the United States and limited deployment potential in other regions. The study concludes that innovative rail transportation solutions combined with advanced rotor technologies can provide a feasible alternative to segmentation and support continued LCOE reductions in the U.S. land-based wind energy market.

1. Introduction

In the U.S. land-based wind energy market, the average rotor diameter has increased steadily during the past 20 years to 115.6 m in 2018 [1]. Although impressive, this average is dwarfed by the recent global land-based turbine platform introductions, such as the GE 5.3-MW Cypress turbine with a 158-m rotor, the Vestas 5.6-MW EnVentus turbine with a 162-m rotor, and the SGRE 5.8-MW turbine with a 170-m rotor. The fact that most new 5-MW class turbines offer a segmented blade option, however, indicates that the costs associated with transporting one-piece blades in excess of 75 m are becoming prohibitive in many markets and could limit further benefits in the levelized cost of energy (LCOE) from going to larger machines. Segmentation, although clearly a component of the overall global deployment strategy, is not the only solution to mitigating escalating land-based blade transportation costs. The U.S. Department of Energy (DOE) Wind Energy Technologies Office (WETO) held a Supersized Wind Turbine Blades Workshop in Washington, D.C., from March 6–7, 2018, to identify additional pathways that could enable continued reduction in LCOE and increased U.S. market expansion. Representatives from the wind turbine supply chain identified on-site manufacturing and innovative transportation, such as airships and controlled blade bending, as alternative potential pathways [2]. The workshop launched the Big Adaptive Rotor (BAR) project.

Content from this work may be used under the terms of the Creative Commons Attribution 3.0 licence. Any further distribution of this work must maintain attribution to the author(s) and the title of the work, journal citation and DOI.
Published under licence by IOP Publishing Ltd

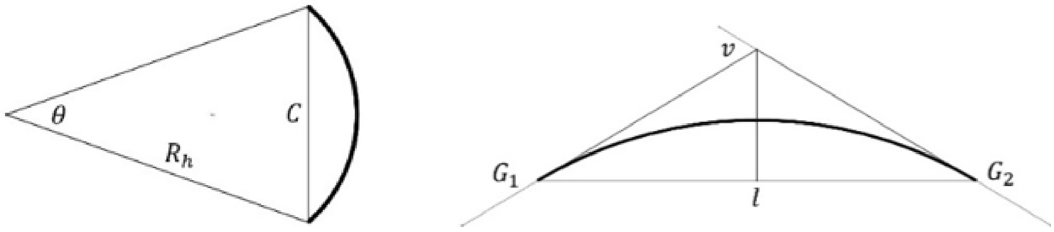

Figure 1. Geometries of horizontal (left) and vertical (right) curves.

The BAR project, funded by DOE WETO, investigates low specific power land-based rotor technologies that can further decrease LCOE and enable nationwide deployment. The baseline turbine for the program is a 5-MW turbine with a specific power of 150 W/m^2 and 100-m long blades. The work presented in this paper is performed under the BAR project and investigates the potential of innovative transportation solutions—specifically, controlled blade bending on U.S. rail infrastructure—to deploy a 100-m one-piece blade from a centralized manufacturing facility to land-based wind turbine sites.

2. Methodology

Wind turbine blades are routinely deployed to wind sites using U.S. rail infrastructure. Historically, blades have been transported rigidly—i.e., no bending is induced in the structure. The next subsections discuss the technical basis used to enable the transport of supersized blades via controlled blade bending.

2.1. Horizontal and Vertical Curvatures

Horizontal curves on U.S. rail lines are measured in degrees of curvature (θ), where the degree of horizontal curvature is defined by the central angle of a curve subtended by a chord (c) of 30.48 m (100 ft), as shown in Fig. 1.

The radius of the horizontal curvature (Rh) is calculated using [3]:

$$R_h = \frac{c}{2 \cdot \sin\left(\frac{\theta}{2}\right)} \tag{1}$$

Vertical curves, both sag and summit, on U.S. rail lines are defined by an entry gradient (G_1) in percentage of vertical feet of rise over a 100-ft horizontal distance, an exit gradient (G_2) in percentage of vertical feet of rise over a 100-ft horizontal distance, the distance between entry and exit gradients (l) in 100-ft stations, and the average change in gradient (v/l) per 100-ft station, as shown in Fig. 1.

Geometrically, vertical curves are parabolic; however, for simplicity, an equivalent circular approximation is used in this study [4]. The radius of the equivalent circular vertical curvature (R_v) is calculated using:

$$R_v = \frac{100 \cdot l}{|G_2 - G_1|} \tag{2}$$

where:

$$l = \frac{|G_2 - G_1|}{\frac{v}{l}} \tag{3}$$

Horizontal and vertical curves vary greatly throughout the U.S. rail network because of varying terrain and infrastructure. To assess regional deployment potential, the maximum

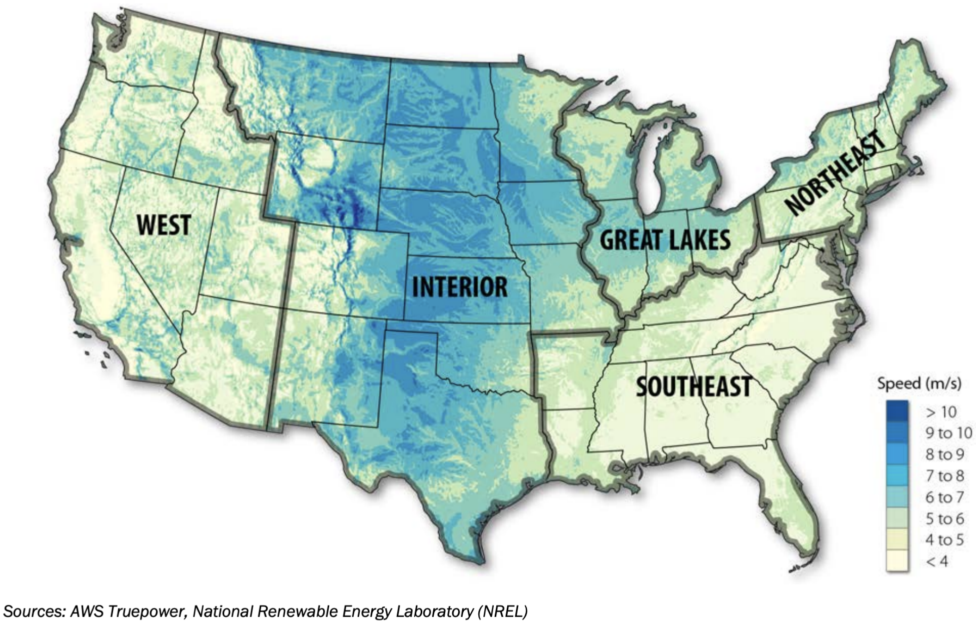

Figure 2. U.S. land-based wind regional boundaries [1].

horizontal and vertical curvature is defined at the regional level in the U.S. land-based wind market, as shown in Fig. 2 [1]. The individual regions are defined as the Interior (i.e., Texas and the Great Plains), West (i.e., Pacific Northwest and California), Great Lakes, Southeast, and Northeast.

The horizontal curvature design criteria to enable limited deployment of blades on main line routes in the Interior region is assumed to be 8 degrees. The design criteria to enable maximum deployment of blades on main line routes in the Interior and limited deployment on main line routes in the West, Great Lakes, Northeast, and Southeast regions is instead set to 13 degrees. The design criteria to enable maximum deployment of blades on main line routes in all regions as well as in industrial yards and ports is set to 23 degrees [5].

The vertical curvature design criteria to enable maximum deployment of blades on main line routes in all regions as well as in industrial yards and ports is set to an equivalent circular radius of 609.6 m (2,000 ft) for both sag and summit curves. This assumes an entry and exit gradient of $\pm$ 1.5% and an average change in gradient of 0.05.

2.2. Clearance Profile

Loads and equipment that fit within standardized clearance profiles—such as AAR Plate C [6], which is roughly 4.72-m (15-ft, 6-in) high by 3.25-m (10-ft, 8-in) wide, as measured from the top center of the rail—are routinely cleared by the railroad and operate relatively unrestricted on the rail network. Oversized loads, as defined by BNSF Railway Company (BNSF) [7] and Union Pacific Railroad [8], are dimensional loads that exceed 3.35 m (11 ft) in width, or 5.18 m (17 ft) in height, or extend beyond the end sills of the flatcar, or exceed a gross rail load (GRL) of 129,727 kg (286,000 lbs) for a 4-axle flatcar or 217,724 kg (480,000 lbs) for an 8-axle flatcar. Oversized loads, such as a 100-m blade, must go through a strict dimensional clearance process and are typically restricted from sections of the rail network. As such, there are no standardized oversized profiles. The clearance profile developed for this study is based on the maximum potential distances controlled by the rail lines as described in guidelines from BNSF and Union Pacific Railroad [9, 10]. Specifically, the clearance profile is defined as a box that is

Data	Imperial	S.I.
Clearance - vertical profile	23 ft	7.01 m
Clearance - horizontal profile	22 ft	6.71 m
Flatcar - deck width	9 ft	2.74 m
Flatcar - deck height	4 ft	1.19 m
Flatcar - length	89 ft	27.13 m
Flatcar - coupler to coupler length	94 ft	28.65 m
Flatcar - truck center to truck center length	66 ft	20.12 m
Flatcar - mass	68,000 lbm	30,844.26 kg
Flatcar - gross rail load 4-axle	286,000 lbm	129,727.31 kg
Flatcar - gross rail load 8-axle	480,000 lbm	217,724.16 kg

Table 1. Flatcar and clearance profile data.

7.01-m (23-ft) high and 6.706-m (22-ft) wide as measured from the top center of the rail. The blade, flatcar, and blade rail transport tooling must always stay within the clearance profile. Clearance profile dimensions and flatcar specifications are listed in Table 1.

2.3. Wheel-Rail Interaction

Bending a wind turbine blade during rail transport generates reaction forces on both the flatcar wheels and track that must be controlled to avoid derailment and track damage. For blade bending forces created in horizontal curves, wheel flange derailment criteria are used to assess potential derailment and track damage. This study takes a simplified approach to railcar dynamics and uses the Nadal L/V ratio criteria to develop an allowable design [11, 12]. The Nadal equation factors the lateral wheel-rail contact force (L), the vertical wheel-rail contact force (V), the flange contact angle (δ), and the coefficient of friction (μ), and it is expressed as:

$$L/V = \frac{\tan\delta - \mu}{1 + \mu \cdot \tan\delta} \tag{4}$$

A coefficient of friction of 0.5 and a flange contact angle of 65 degrees are used to derive a Nadal value of 0.8. It is assumed that train speeds are extremely slow—i.e., there are no additional accelerations besides gravity—and that the total lateral and vertical forces acting on the flatcar are distributed equally among all wheels. By assuming an additional rail transport safety factor of 1.6, an allowable design L/V ratio of 0.5 is adopted.

For blade bending forces created in sag and summit vertical curves, wheel lift and GRL exceedance are used to assess potential derailment and track damage. Vertical forces that act to lift the flatcar wheels off the rail require the wheels to maintain at least 10% of the static downward force [12]. Vertical forces that act to drive the flatcar wheels down into the rail require that the GRL is not exceeded. It is again assumed that train speeds are extremely slow—i.e., there are no additional accelerations besides gravity—and that the total lateral and vertical forces acting on the flatcar are distributed equally among all wheels.

2.4. Blade Strains

Standard flatcars have a coupler-to-coupler length of 28.65 m (94 ft), see Table 1. It is assumed that the 100-m long blades are positioned across four flatcars, with the root of the blade positioned in the center of the first flatcar. The chord is assumed to be aligned in the vertical direction at zero twist angle, and the trailing edge points upward. As the blade navigates horizontal and vertical curves, blade strains resulting from bending are considered at the farthest distance from the neutral axis in the train coordinate system. The design allowable strain for blade bending during transport is derived by taking the characteristic ultimate compressive strain in the laminates and dividing it by a combined material safety factor of 2.977 [13] and an additional rail transport safety factor of 1.5.

2.5. Reaction Forces and Moments

This study models the blade as a Euler-Bernoulli cantilever beam with the root located in the middle of the first flatcar and the beam supported by rolling boundary conditions along the blade span. The blade is assumed to be subjected to distributed loading q to keep it within the clearance profile. From q, the beam internal shear forces (S) are computed by integrating q along blade span r:

$$S = \int q \, dr \tag{5}$$

S are in turn integrated along the blade span to compute the bending moments:

$$M = \int S \, dr \tag{6}$$

From M, the longitudinal strains ϵ are estimated at the locations y, which correspond to the distance between the neutral axis and the material farthest from it in the rail reference system:

$$\epsilon = \frac{M \cdot y}{EI} \tag{7}$$

where EI represents the blade stiffness, which is flapwise for the horizontal curves and edgewise for the vertical curves.

The model assumes that q is nonnegative—i.e., all flatcars pull the blade into the clearance profile, and no complex push/pull loading is allowed. The highest reaction force and moment of the cantilever beam are consequently experienced by the first flatcar. Given S and M at the blade root, the lateral reaction force at the front wheel set of the first flatcar (L_{1f}) is calculated as:

$$L_{1f} = 0.5 * S_0 + \frac{M_0}{L_x} \tag{8}$$

where L_x is the distance between wheel sets (see Table 1), and S_0 and M_0 are the forces and moments, respectively, at the blade root. L_{1f} is then divided by the vertical force V acting on the wheel set, which is assumed here to be half of the GRL of the flatcar; and the ratio is compared to the maximum allowable L/V value of 0.5. This computation assumes that additional counterweight mass as well as 8-axle flatcars can be used to bring the L/V ratio within the allowable range without exceeding the GRL.

For vertical curvatures, the vertical reaction V_{1f} acting on the front wheel set of the first flatcar is computed in the same manner as L_{1f} in Eq. 8. The total vertical force (V) is calculated by summing V_{1f} with the forces attributed to the blade mass, the tooling mass, the flatcar mass, and an additional counterweight mass. If the vertical upward force indicates wheel lift, additional counterweight mass and 8-axle flatcars are used to achieve at least 10% of the static downward force without exceeding the GRL [12]. If the vertical downward force indicates instead GRL exceedance, 8-axle flatcars are used.

The model also assumes that a hydraulic system has the ability to dynamically adjust the vertical position of the blade root and the horizontal and vertical angles between the blade pitch axis at the blade root and the flatcar. As discussed in Sect. 3, this greatly reduces the blade strains and reaction forces. Complex track curvatures, such as S-turns or combinations of horizontal and vertical rail curvatures, are not considered by the model. The additional cost of an 8-axle flatcar or the additional route restrictions—caused by, for example, older incompatible rail lines or bridge or truss structures—are also not considered.

2.6. Systems Engineering Framework

The rail transport model is implemented in the Wind Integrated System Design and Engineering Model (WISDEM) framework [14]. WISDEM is a multifidelity design framework for wind turbines and wind plants implemented in Python. WISDEM is fully open-source, and it is based on the multidisciplinary design, analysis, and optimization library OpenMDAO [15]. Many different design studies can be performed in WISDEM thanks to its modularity. In this study, the rail model is coupled to the rotor design module of WISDEM, which is set up to run an aerostructural design optimization of wind turbine blades to minimize a user-defined merit figure, such as blade mass, maximum tip deflection, or LCOE. The design variables parametrize blade twist, chord, and the internal thickness of the spar caps along the blade span.

The rail module is implemented to run a nested optimization to verify that the blade can navigate the horizontal and vertical curves without exceeding the maximum strains. The design variables in the suboptimization routine perturb q along the blade span, the angles at the blade root, and the vertical position of the blade root. The optimization is constrained to limit the strains (ϵ) to stay within the maximum allowable range and to keep the blade within the clearance profile for the horizontal and vertical curvatures. The figure of merit of the optimization problem is L_{1f}. If the nested optimizer finds a solution, the L/V ratio is estimated and passed as a constraint to the outer design loop. If the nested optimizer is not able to keep the blade within the clearance profile without exceeding the maximum strains, the constraint on the L/V ratio is artificially imposed as violated.

3. Results

Within the BAR project, a reference wind turbine, named BAR00, was designed using WISDEM [14]. The rotor has cone and tilt angles of 4 and 6 degrees, respectively, and a tip speed ratio of 10.5. The BAR00 blade has a mass of 65,000 kg, two spar caps made of unidirectional glass fiber-reinforced plastic, two shear webs, a maximum chord of 5.3 m, and a prebend of 4 m. The BAR00 blade was designed without specific logistic constraints, and the prebend and maximum chord are found limiting the rail transport to horizontal curves up to 6 degrees.

WISDEM has been run to redesign the BAR00 blade imposing that the blade must be able to navigate horizontal curvatures up to 13 degrees and vertical curvatures up to 2,000 ft of radius with up to 8-axle flatcars. During the design process, the chord is constrained to 4.75 m, and the prebend is removed. These assumptions help relax the transportation constraints. Chord and spar cap thickness are parametrized at eight locations along the blade span, and the maximum tip deflection is no longer imposed as a constraint, whereas it is adopted as a figure of merit to be minimized. In terms of maximum allowable strains, an upper limit for the unidirectional laminates during turbine operation is set at 5,000 microstrains, whereas during blade transport the limit is reduced to 3,500 microstrains. These values are determined given the ultimate compressive strain of 1.53% for unidirectional glass fiber-reinforced plastic laminates based on Vectorply E-LT-5500 glass fiber and epoxy resin [13, 16]. Once the optimizer converges, a quick aerodynamic optimization is performed to bring back the twist and the tip speed ratio to their aerodynamic optima.

The resulting design, named BAR01, is compared to the conventional BAR00 in Fig. 3. The optimized blade is significantly lighter and more flexible than the BAR00 design. The mass of the BAR01 blade is 51,400 kg, and the tip deflection during operation is estimated to be increased by 40%. This suggests that the blade BAR01 might be a viable solution only in a downwind rotor configuration. In terms of natural frequencies, the BAR01 has the first flapwise frequency equal to 0.35 Hz and the first edgewise frequency equal to 0.48 Hz, whereas the 3P frequency is equal to 0.39 Hz. The rotor is therefore a soft rotor, which will require a careful assessment of the aeroelastic behavior, especially in a downwind configuration where the 3P

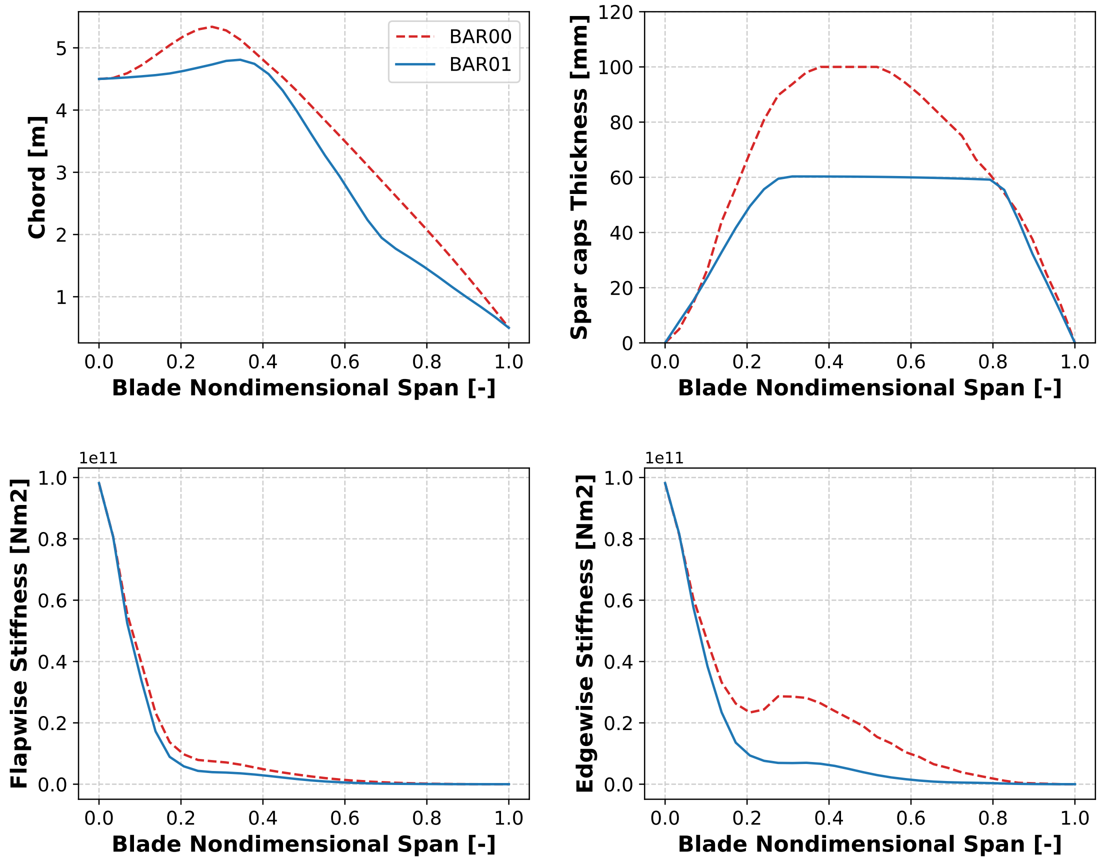

Figure 3. Comparison of the reference blade design (BAR00) to the design optimized for rail transport (BAR01).

Degrees of horizontal curvature	**5**	**8**	**11**	**13**
Curvature radius R_h [m]	349.4	218.5	159.6	134.6
Rigid rotation root [deg]	6.9	8.6	9.9	10.5
L_{1f} [kN]	0.0	99.5	305.3	528.4
L/V 4-axle [-]	0.0	0.16	0.48	0.83
L/V 8-axle [-]	0.0	0.09	0.29	0.50

Table 2. Blade root angle, lateral reaction forces, and L/V ratios at four angles of horizontal curvatures.

component of the loads might be increased by the rotor-tower interactions.

The next subsections investigate the parameters of rail transport for the horizontal and vertical curvatures.

3.1. Horizontal Curve Analysis

The horizontal curve analysis returns that the blade BAR01 can navigate turns up to 16 degrees without exceeding the maximum strain limits. Nonetheless, the reaction forces on the first flatcar exceed the maximum allowable L/V ratio right above 11 degrees of horizontal curve with a 4-axle flatcar and above 13 degrees of horizontal curve assuming an 8-axle flatcar. Table 2 reports the values of blade root angle, lateral reaction forces, and L/V ratios, and Fig. 4 shows the deformed shapes for the horizontal curves of 5, 8, 11, and 13 degrees.

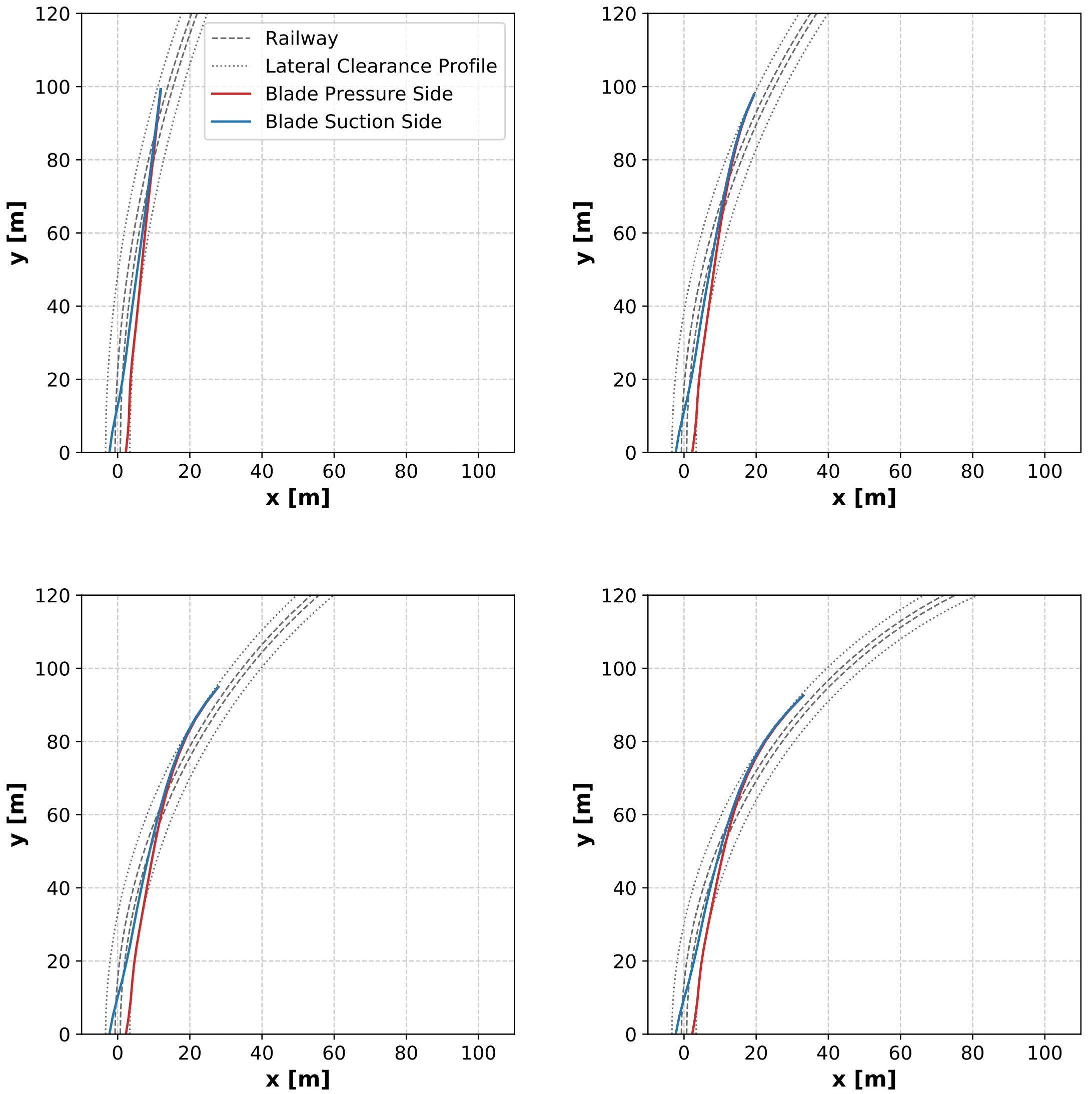

Figure 4. Birds-eye view of the deformed blade configurations for horizontal curves of 5 (top left), 8 (top right), 11 (bottom left), and 13 (bottom right) degrees.

3.2. Vertical Curve Analysis

During sag and summit vertical curves, the BAR01 blade needs to bend in the edgewise direction (see Fig. 5), and the sag curves are found to be more challenging because of the trailing-edge orientation. The reaction forces on the first flatcar generated by blade bending are reported in Table 3. The summit curve generates an upward lifting V_{1f} of 37.8 kN on the front wheel set of the first flatcar, whereas the sag curve generates a downward rail contact force of 168.9 kN. The resulting net reaction forces—inclusive of flatcar, tooling, and counterweights—are downward and well spaced between the 10% static downward force and the maximum allowable GRL force of 1,272.6 kN for a 4-axle flatcar. It is therefore concluded that the BAR01 blade can navigate vertical curvatures of a 2,000-ft radius without lifting flatcars or damaging the rail track.

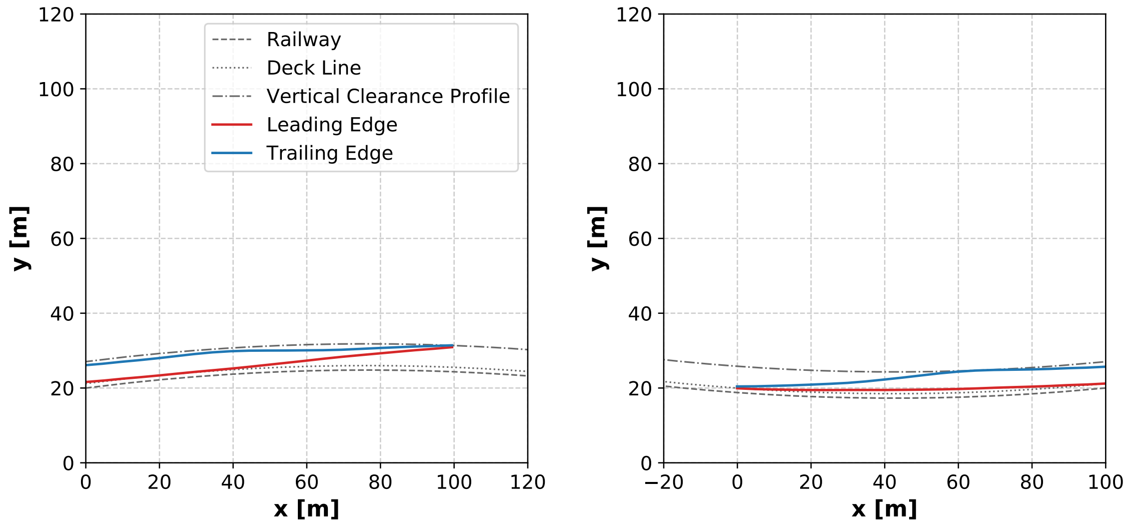

Figure 5. Side view of the deformed blade configurations for summit (left) and sag (right) vertical curves with a 2,000-ft curvature radius.

	Summit	**Sag**
Vertical radius R_v [m]	609.6	609.6
Rigid root rotation [deg]	2.8	2.4
Rigid root vertical displacement [m]	0.3	0.0
V_{1f} [kN]	-37.8	+168.9

Table 3. Blade root angle, vertical displacement of blade root, and vertical reaction forces for a vertical curvature radius of 2000 ft. Negative V_{1f} indicates a lifting force, whereas positive V_{1f} indicates a downward rail contact force. Resulting net forces are found to not limit rail transport.

4. Conclusions and Future Work

This work presents a study on the transportability of 100-m long wind turbine blades across the U.S. rail system via controlled blade flexing. A conventional design, named BAR00, is found to violate the transportation constraints and is found to be not transportable on rail. An alternative design, named BAR01, is investigated in terms of clearance, curvatures, and reaction forces. The BAR01 blade is assessed as having deployment potential along the main rail lines of the United States for horizontal curvatures up to 13 degrees. Vertical curvatures up to 2,000-ft radius are found not to be limiting.

Overall, the study concludes that within the U.S. land-based market, coordinated advancements in blade design and rail transport tooling have the potential to extend the deployment of one-piece blade lengths into the 100-m range. The current designs, however, push the current state of the art in terms of blade compliance, and an in-depth investigation into the aero-servo-elastic behavior of rail-transportable blades, such as increased torsional deformations and reduced flutter margins, is ongoing. The preliminary results are promising. Downwind rotor configurations are part of the analysis and will be compared to equivalent upwind configurations in terms of costs and performance. Advanced wind turbine system design and optimization processes that integrate rail logistic constraints and transport load cases directly into the blade design and certification process are suggested.

Future work should also include a detailed techno-economic analysis to assess the regional

LCOE reduction potential of rail transport with blade flexing. The analysis should address rail transport costs, including tooling and load monitoring; rail line routing details; scalability; last-mile delivery; fatigue life impact; and the costs associated with additional rail transport design load cases and blade certification. The optimized rotor technologies based on controlled blade flexing on the U.S. rail system should be compared, on a cost basis, to alternative solutions, such as segmentation and on-site manufacturing, to provide forward guidance on which technologies or combination of technologies can enable the largest LCOE reductions and market opportunities on a regional basis.

Acknowledgments
The authors would like to acknowledge the valuable input provided during the writing of this paper. The authors are grateful to Clay Gambill, Chris King, and John Ferris at BNSF Logistics, and Nick Johnson at National Renewable Energy Laboratory. Their feedback, guidance, and review are appreciated. This work was authored by the National Renewable Energy Laboratory, operated by Alliance for Sustainable Energy, LLC, for the U.S. Department of Energy (DOE) under Contract No. DE-AC36-08GO28308. Funding provided by the U.S. Department of Energy Office of Energy Efficiency and Renewable Energy, Wind Energy Technologies Office. The views expressed in the article do not necessarily represent the views of the DOE or the U.S. Government. The U.S. Government retains and the publisher, by accepting the article for publication, acknowledges that the U.S. Government retains a nonexclusive, paid-up, irrevocable, worldwide license to publish or reproduce the published form of this work, or allow others to do so, for U.S. Government purposes.

References
[1] Wiser R, Bolinger M. 2018 Wind Technologies Market Report. U.S. Department of Energy Technical Report, pp: 2-24. DOE/GO-102019-5191, August 2019.
[2] DNV/GL, Creating Pathways to Success for Supersized Wind Turbine Blades: 2018 Workshop Summary Report. Document No. 10080081-HOU-R-10-C, 01 May 2018.
[3] CSX, Standard Specifications for the Design and Construction of Private Sidetracks, 2016. `www.csx.com`
[4] TMR, 2004. Chapter 12: Vertical Alignment. Road Planning and Design Manual (1st Ed.). pp: 23-24. Department of Transport and Main Roads. Queensland, Australia.
[5] Landrum SC, King TC. Wind Turbine Blade Railroad Transportation with Two Axis Translation. US9315200 B1, United States Patent and Trademark Office, 19 April 2016.
[6] Association of American Railroads, Manual of Standards and Recommended Practices, Section C, Car Construction Fundamentals and Details. Standard 2028, Plate C - Equipment Diagram for Limited Interchange Service, 2013.
[7] BNSF Railway Company, Machinery & Oversized. `https://www.bnsf.com/ship-with-bnsf/industrial-products/machinery-and-oversized/`
[8] Union Pacific Railroad, Dimensional Shipping Made Easy. `https://www.up.com/customers/ind-prod/consumer/machdimen/seven_steps/index.htm`
[9] BNSF Railway Company. Guidelines for Industry Track Projects. August 2018.
[10] Union Pacific Railroad. Guidelines for Railroad Grade Seperation Projects. January 2016.
[11] Weinstock H. Wheel Climb Derailment Criteria for Evaluation of Rail Vehicle Safety. ASME Paper 84-WA/RT-1. Presented at 1984 Winter annual meeting, Phoenix, AZ, 1984.
[12] Federal Register, Vol. 61, No. 117, p: 30688, 1996.
[13] Griffith D, Resor BR, Ashwill T. Large Offshore Rotor Development: Design and Analysis of the Sandia 100-meter Wind Turbine Blade. 53rd AIAA/ASME/ASCE/AHS/ASC Structures, Structural Dynamics and Materials Conference, April 2012.
[14] `https://github.com/WISDEM/WISDEM`
[15] Gray JS, Hwang JT, Martins JRRA, Moore KT, Naylor BA. OpenMDAO: An Open-Source Framework for Multidisciplinary Design, Analysis, and Optimization. Structural and Multidisciplinary Optimization, 2019.
[16] DOE / MSU Composite Material Fatigue Database, March 31, 2010, Version 19.0.